Constituents of *Amoora cucullata* with TRAIL resistance-overcoming activity†

Firoj Ahmed,[a,b] Kazufumi Toume,[a] Samir K. Sadhu,[b] Takashi Ohtsuki,[a] Midori A. Arai[a] and Masami Ishibashi*[a]

Received 6th April 2010, Accepted 3rd June 2010
First published as an Advance Article on the web 23rd June 2010
DOI: 10.1039/c004927a

In search of bioactive natural products for overcoming TRAIL resistance from natural resources, we previously reported a number of active compounds. Bioassay-guided fractionation of mangrove, *Amoora cucullata*, collected from Sundarbans Mangrove Forest, Bangladesh, led to the isolation of four new compounds (**1–4**), along with seven known compounds (**5–11**). Of the isolates, compounds **1**, **5**, **8**, and **9** showed TRAIL resistance-overcoming activity, among which **8** showed the most potent activity and enhanced TRAIL-induced apoptosis in TRAIL-resistant human gastric adenocarcinoma (AGS) cells through the activation of caspase-3/7, enhancing the expression of DR4 and DR5 mRNA in AGS cells. Cell death caused by the combined treatment of **8** and TRAIL was inhibited by human recombinant DR5/Fc and DR4/Fc chimera proteins, indicating that **8** sensitizes TRAIL-resistant AGS cells to TRAIL through the induction of DR4 and DR5.

Introduction

Tumor necrosis factor (TNF)-related apoptosis-inducing ligand (TRAIL) is a promising anticancer agent as it can selectively kill tumor cells.[1] The *in vivo* administration of TRAIL has been proved to be safe, unlike the other members of the TNF superfamily. It is well-known that there are two essential apoptotic pathways, referred to as the death-receptor (extrinsic) pathway and the mitochondrial (intrinsic) pathway. TRAIL can activate either pathway, depending on the cell type. TRAIL-induced apoptosis initiated by the death-receptor pathway involves death receptor (DR) engagement, death-inducing signaling complex (DISC) formation, proteolytic activation of caspase-8, and, consequently, activation of caspase-3. Proteolytic caspase-8 further activates Bid, which, in turn, translocates to the mitochondria and activates the mitochondrial pathway;[1] however, it has become a problem that considerable numbers of cancer cells, especially some highly malignant tumors, are resistant to apoptosis induction by TRAIL.[2] Resistance to TRAIL can occur at different points in the signaling pathways of TRAIL-induced apoptosis. Overcoming TRAIL resistance and understanding the mechanisms underlying such resistance are thus very important in anticancer drug discovery.[3,4] Different chemotherapeutic agents, including a number of natural products, are reported to have TRAIL resistance-overcoming activity. For example, luteolin is a naturally occurring flavone that induces apoptosis in various cancer cells.[5] Similarly, phytochemicals, such as curcumin, resveratrol, and indole-3-carbinol, have received attention recently as anticancer agents, since it was reported that they augment TRAIL-mediated apoptosis in cancer cells.[1]

As part of the continued research program into the isolation of bioactive compounds for overcoming TRAIL resistance,[6] we explored medicinal plants from Bangladesh. After initial screening of the extracts library, MeOH extract of leaves of *Amoora cucullata* (Meliaceae) was found to be potently active in overcoming TRAIL resistance. *Amoora cucullata* Roxb. (syn.: *Aglaia cucullata* Roxb.) is a tall tree, grown in the coastal forests of Bengal, Burma, Malay peninsula, Andamans, and Borneo. It was collected from the Sundarbans Mangrove Forest, Bangladesh, where it is known as 'Amoor', 'Latmi', and 'Natmi' among the local people. Its leaves are traditionally used in the treatment of inflammation.[7] Juice of the leaves is antibacterial and extensively used for the treatment of dysentery, skin diseases and in cardiac diseases.[8] Crude MeOH extracts of leaves were reported to show anti-inflammatory, antinociceptive, diuretic, and CNS depressant activities.[9,10] Previous chemical investigation of its leaves isolated polyphenols and tannins, whereas from its fruits, several rocagloic acid derivatives were isolated.[11] Bioassay-guided fractionation of MeOH extracts of its leaves led to the isolation of four new compounds (**1–4**) along with seven known compounds (**5–11**). Here, we report the isolation and structural elucidation of compounds **1–4**, along with the TRAIL resistance-overcoming activity of the isolates. We also describe the sensitizing effect of **8**, the most potent compound, to TRAIL-induced apoptosis by upregulation of DR4 and DR5 in TRAIL-resistant human gastric adenocarcinoma (AGS) cell lines.

Results and discussion

The MeOH extract of leaves of *A. cucullata* was partitioned between hexane, EtOAc and BuOH, followed by repeated column chromatography and preparative HPLC to afford compounds **1–11** (Fig. 1).

Compound **1** was isolated as an optically active, colorless solid, and was assigned the molecular formula $C_{36}H_{40}N_2O_9$ on

[a]*Graduate School of Pharmaceutical Sciences, Chiba University, 1-33 Yoyoi-cho, Inage-ku, Chiba 263-8522, Japan. E-mail: mish@p.chiba-u.ac.jp; Fax: +81-43-290-2913; Tel: +81-43-290-2913*
[b]*Pharmacy Discipline, Life Science School, Khulna University, Khulna-9208, Bangladesh*

† Electronic supplementary information (ESI) available: NMR spectra. See DOI: 10.1039/c004927a

Table 1 ^{1}H and ^{13}C NMR data of **1** in $CDCl_3$

Position	δ_C	δ_H (J in Hz)
2	86.3	
3	47.7	4.00 (s)
4	56.3	3.73 (s)
5	83.7	
5a	104.4	
6	158.3	
7	92.8	5.99 (d, 2.4)
8	161.3	
9	93.4	5.44 (d, 2.4)
9a	154.0	
10	90.5	
11	174.0	
13	38.6	3.30 (m); 2.22 (m)
14	25.6	1.50 (2H, m)
15	26.8	1.50 (2H, m)
16	39.3	3.30 (2H, m)
18	169.3	
19	133.1	
20	133.2	6.30 (dt, 12.2, 6.1, 1.3)
21	59.5	4.21 (2H, dd, 6.1, 1.3)
22	13.1	1.80 (3H, d, 1.2)
1′	128.6	
2′/6′	128.7	7.61 (2H, d, 8.8)
3′/5′	113.7	6.99 (2H, d, 8.8)
4′	159.9	
1″	135.3	
2″/6″	127.1	6.68 (2H, m)
3″/5″	127.1	6.92 (2H, m)
4″	125.8	6.92 (m)
OMe-6	56.1	3.89 (3H, s)
OMe-8	55.3	3.48 (3H, s)
OMe-4′	55.3	3.86 (3H, s)

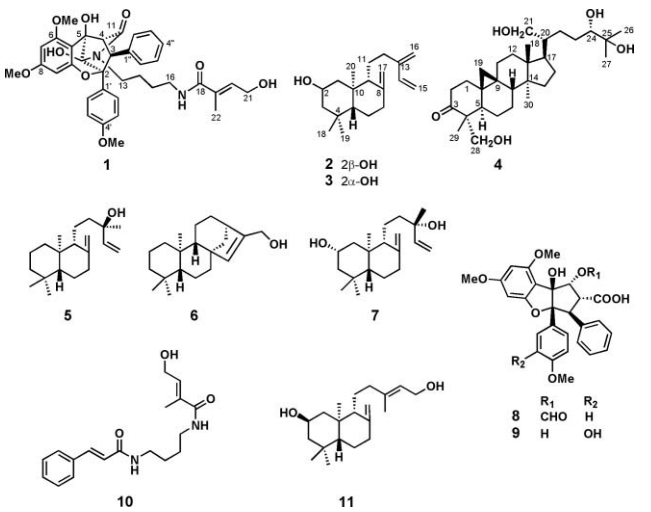

Fig. 1 Chemical structures of compounds **1–11** from *A. cucullata*.

the basis of HRESIMS at m/z 667.2601 $[M + Na]^+$ (Calcd. for $C_{36}H_{40}N_2O_9Na$, 667.2626, Δ –2.5 mmu), and ^{1}H and ^{13}C NMR spectroscopic data. Its IR spectrum showed the presence of hydroxyl (3362 cm^{-1}) and carbonyl (1684 cm^{-1}) groups. The ^{1}H and ^{13}C NMR data (Table 1) showed the presence of thirteen quaternary carbons, including two amide carbons (δ_C 169.3 and 174.0), fourteen methines, five methylenes, one methyl, and three methoxy groups. In the ^{1}H NMR spectrum, signals for three methoxy groups at δ_H 3.48, 3.86, and 3.89 were found. In addition, signals for three aromatic rings, similar to those of compound **8**, were observed; that is, two *meta* coupled aromatic protons at δ_H 5.44 (d, J = 2.4 Hz) and 5.99 (d, J = 2.4 Hz) indicated a 1,2,3,5-tetrasubstituted benzene ring (ring A) fused to the oxaheptane ring (ring B), the characteristic AA′BB′ system of a *p*-disubstituted benzene ring (ring D) at δ_H 6.99 (2H, d, J = 8.8 Hz) and δ_H 7.61 (2H, d, J = 8.8 Hz), and the signals of a monosubstituted benzene ring (ring C) (δ_H 6.68, 2H, m; δ 6.92, 3H, m). Furthermore, two methines at δ_H 4.00 (s, H-3) and 3.73 (s, H-4) were assigned to ring B, typical of a cyclopenta[b]benzopyran skeleton.[12] Close inspection of ^{1}H and ^{13}C NMR data as well as HMBC correlations (Fig. 2A), and comparison with the spectral data of compound **10**, also indicated the presence of the hydroxytigloyl-1,4-butanediamide (HTBD) moiety, forming an amide linkage with carbonyl C-11 (δ_C 174.0), which was supported by the HMBC correlation between H_2-13 of the HTBD moiety and C-11. The connectivity of rings C, D, and the HTBD moiety to ring B was assigned on the basis of HMBC correlations. In the HMBC spectrum, a cross peak was observed from δ_H 7.61 (2H, d, J = 8.8 Hz, H-2′/6′) to δ_C 86.3 (C-2), indicating that ring D was connected to C-2. HMBC correlation from H-3 (δ_H 4.00, s) to C-2″/6″(δ_C 127.1) indicated that ring C was connected to C-3. HTBD moiety was connected to C-4 on the basis of HMBC correlations from both H-3 and H-4 to C-11 of the HTBD moiety (Fig. 2A). Further HMBC correlations from H-3 to C-2, C-4, and C-10, and from H-4 to C-2, C-5, C-5a, and C-10, supported the structure of the tricyclic ring moiety. It was evident from the ^{1}H and ^{13}C NMR spectra that C-10 (δ_C 90.5) was a quaternary carbon containing a hydroxyl group, and N-12 of the putrescine (1,4-butanediamide) moiety formed a bond with C-10 to create a five-membered cyclic amide, forming a cyclopenta[b]benzopyran skeleton similar to that of cyclofoveoglin isolated from *Aglaia foveolata*.[12] Thus, the structure of **1** was similar to that of cyclofoveoglin with a difference in the butanediamide side chain; the benzoyl moiety of the benzoyl-1,4-butanediamide side chain of cyclofoveoglin was replaced with a hydroxytigloyl moiety forming a hydroxytigloyl-1,4-butanediamide in **1**.

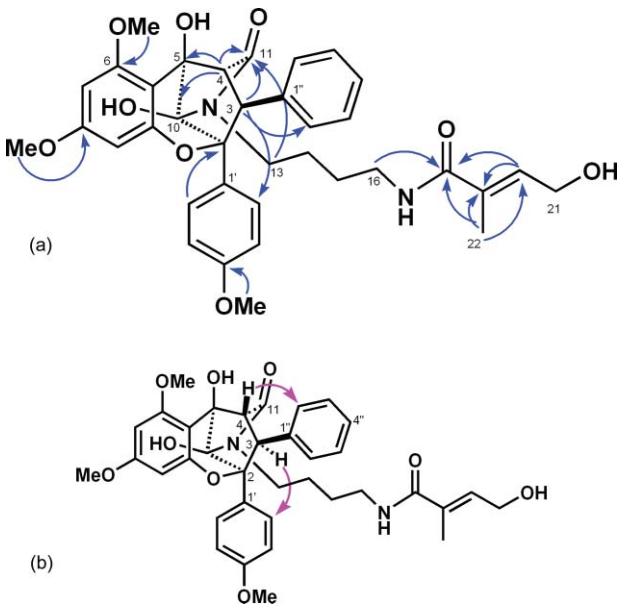

Fig. 2 (A) Key HMBC (arrows) correlations. (B) Selected NOE experiments of compound **1**.

Table 2 ^{1}H and ^{13}C NMR data of **2** and **3** in $CDCl_3$

	2		**3**	
Position	δ_C	δ_H (J in Hz)	δ_C	δ_H (J in Hz)
1	48.1	2.06 (1H, m) 0.95 (1H, m)	45.8	1.74 (1H, dd, 14.0, 5.2) 1.52 (1H, dd, 14.0, 5.2)
2	65.7	3.82 (1H, tt, 11.4, 4.1)	67.9	4.14 (1H, quintet, 5.2)
3	51.1	1.74 (1H, m) 1.12 (1H, t, 12.0)	46.7	1.62 (1H, m) 1.45 (1H, dd, 14.0, 3.3)
4	35.0		33.0	
5	54.9	1.07 (1H, dd, 12.4, 2.8)	53.2	1.16 (1H, dd, 12.4, 2.8)
6	23.9	1.28 (1H, m) 1.25 (1H, m)	24.5	1.74 (1H, dd, 14.0, 5.2) 1.39 (1H, dd, 12.9, 4.1)
7	38.1	1.98 (1H, m) 2.39 (1H, m)	38.1	1.97 (1H, m) 2.38 (1H, m)
8	147.7		147.9	
9	56.4	1.67 (1H, m)	57.1	1.62 (1H, m)
10	41.0		39.6	
11	22.5	1.70 (2H, m)	22.8	1.62 (1H, m) 1.57 (1H, m)
12	30.1	2.35 (1H, m) 1.98 (1H, m)	30.3	2.38 (1H, m) 1.97 (1H, m)
13	146.9		147.1	
14	139.0	6.34 (1H, dd, 17.6, 10.7)	139.1	6.35 (1H, dd, 17.6, 10.8)
15	113.3	5.20 (1H, d, 17.6) 5.02 (1H, d, 10.7)	113.2	5.20 (1H, d, 17.6) 5.02 (1H, d, 10.8)
16	115.6	4.98 (1H, s) 4.96 (1H, s)	115.6	4.98 (1H, s) 4.96 (1H, s)
17	107.2	4.56 (1H, d, 1.4) 4.87 (1H, d, 1.4)	107.0	4.56 (1H, s) 4.86 (1H, s)
18	33.7	0.92 (3H, s)	33.3	0.90 (3H, s)
19	22.6	0.82 (3H, s)	24.6	0.96 (3H, s)
20	15.4	0.70 (3H, s)	17.4	0.90 (3H, s)

The relative stereochemistry of **1** was determined on the basis of NMR data and from NOE correlations (Fig. 2B). In the ^{1}H NMR spectrum, both H-3 and H-4 appeared as singlets, which is possible when the dihedral angle is close to 90°. The model showed that the angle was about 90°. Moreover, NOE correlations between H-3 and H-4, from H-3 to H-2′, and from H-4 to H-2″ were compatible with the proposed structure.

Compound **2** was isolated as an optically active colorless oil, and was assigned the molecular formula $C_{20}H_{32}O$ on the basis of HREIMS at m/z 288.2468 (M^+) (Calcd. for $C_{20}H_{32}O$, 288.2453, Δ +1.5 mmu), and ^{1}H and ^{13}C NMR spectroscopic data (Table 2). The ^{13}C NMR spectrum showed 20 carbon signals, including the signals for three methyls, nine methylenes, four methines and four quaternary carbons. The ^{13}C NMR spectrum included three double bonds (δ_C 147.7, 146.9, 139.0, 115.6, 113.3, and 107.5) and one secondary hydroxyl group at δ_C 65.7. Its ^{1}H NMR spectrum indicated the existence of three tertiary methyl groups at δ_H 0.92, 0.82, and 0.70, corresponding to Me-18, Me-19, and Me-20, respectively, along with three methylene groups at δ_H 5.20 and 5.02 (H_2-15), 4.97 (H_2-16), and at δ_H 4.87 and 4.56 (H_2-17). A triplet–triplet at δ_H 3.82 (J = 11.4 and 4.1 Hz) was also assignable to the hydrogen attached to a hydroxy-bearing carbon at δ_C 65.7, and was unequivocally determined to be located between C-1 and C-3, on the basis of COSY correlation (Fig. 3A). Thus, from the ^{1}H and ^{13}C NMR spectroscopic data along with HMBC correlation data, it was evident that **2** was a labdane diterpene containing the 2β-hydroxy group.[13]

The relative stereochemistry of **2** was assigned on the basis of both coupling constant data and NOE correlations (Fig. 3B). The coupling constant for H-1β/H-2 and H-3β/H-2 was 11.4 Hz,

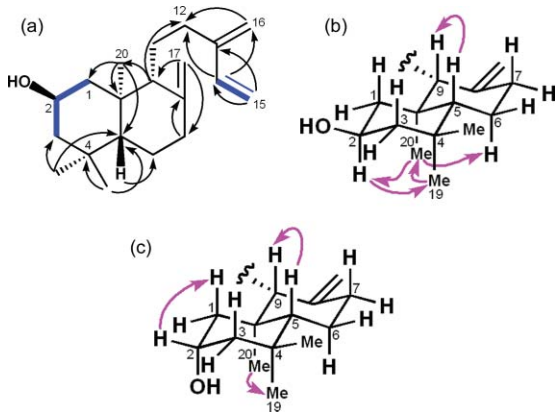

Fig. 3 (A) COSY (bold lines) and key HMBC (arrows) correlations of **2**. (B) Selected NOE correlations (arrows) of **2**. (C) Selected NOE correlations (arrows) of **3**.

while that for H-1α/H-2 and H-3α/H-2 was 4.1 Hz, indicating that H-2 was α-axial. NOE correlations from H-2 to Me-19 and Me-20 indicated the alpha orientation of Me-19 and Me-20. NOE correlations from Me-20 to H-2 and H-6α are also compatible with the proposed configuration. Moreover, NOE correlations between H-5 and H-9 indicated that both H-5 and H-9 were β-oriented; thus, the compound **2** was determined as 2β-hydroxy-labda-8(17),13(16),14-triene.

Compound **3** was isolated as an optically active colorless oil, and was assigned the same molecular formula, $C_{20}H_{32}O$, as **2**, as indicated by HREIMS at m/z 288.2445 $[M]^+$ (Calcd. for $C_{20}H_{32}O$, 288.2453, Δ –0.8 mmu). The ^{1}H and ^{13}C NMR spectroscopic data (Table 2) of **3** were also comparable with those of **2**, with the exception of the signals for H-2, which appeared as a quintuplet at δ 4.14 (J = 5.2 Hz) due to the equatorial–equatorial or equatorial–axial coupling with H-3 and H-1 in **3**, whereas the H-2 of **2** appeared as a triple–triplet at δ_H 3.82 (J = 11.4 and 4.1 Hz). This evidence suggested that **3** was an isomer of **2** differing in the configuration at C-2. In **3**, alpha orientation was assigned for its 2-OH group, and H-2 was assigned as β-equatorial based on its multiplicity pattern and coupling constant value.

The relative stereochemistry of **3** was further assigned on the basis of NOE correlations (Fig. 3C). NOE correlations from H-2 to H-1β, correlations between H-5 and H-9, and between Me-19 and Me-20 are compatible with the proposed configuration; thus, the compound **3** was determined as 2α-hydroxy-labda-8(17),13(16),14-triene. The absolute stereochemistry of compounds **1–3** remained undefined.

Compound **4** was isolated as an optically active colorless solid, and was assigned the molecular formula $C_{30}H_{50}O_5$ on the basis of HRESIMS at m/z 513.3546 $[M + Na]^+$ (Calcd. for $C_{30}H_{50}O_5Na$, 513.3550, Δ –0.5 mmu), and ^{1}H and ^{13}C NMR spectroscopic data (Table 3). Its IR spectrum showed the presence of hydroxyl (3398 cm^{-1}) and carbonyl (1698 cm^{-1}) groups. The ^{13}C NMR data showed the presence of thirty carbons, including five methyls, thirteen methylenes, five aliphatic methines, and seven quaternary carbons, which was confirmed from DEPT spectra. The ^{1}H NMR spectrum displayed signals due to a cyclopropyl methylene (δ_H 0.59 and 0.80, both d, J = 4.2 Hz), five tertiary methyls (δ_H 0.91, 1.00, 1.06, 1.15, and 1.20, each s), a hydrogen attached to a hydroxy-bearing methine carbon group (δ_H 3.35, dd, J = 8.4 and 1.6 Hz),

Table 3 ^{1}H and ^{13}C NMR data of **4** in $CDCl_3$

Position	δ_C	δ_H (J in Hz)
1	33.5	1.86 (dt, 13.9, 3.8) 1.58 (m)
2	38.1	2.71 (dt, 13.9, 6.4) 2.27 (dq, 13.9, 2.3)
3	218.6	
4	54.9	
5	42.6	2.15 (1H, dd, 12.4, 4.2)
6	20.9	1.52 (m), 1.20 (m)
7	28.2	1.32 (m), 1.58 (m)
8	47.7	1.52 (m)
9	21.1	
10	25.5	
11	26.7	2.06 (m), 1.20 (m)
12	31.9	1.52 (m)
13	45.2	
14	48.8	
15	35.4	1.23 (m)
16	25.6	1.23 (m) 1.71 (m)
17	46.5	1.92 (m)
18	18.4	1.02 (3H, s)
19	29.6	0.82 (1H, d, 4.2) 0.60 (1H, d, 4.2)
20	42.7	1.58 (m)
21	62.5	3.77 (1H, dd, 11.2, 3.2) 3.60 (1H, dd, 11.2, 5.2)
22	26.5	1.50 (2H, m)
23	27.7	1.58 (2H, m)
24	78.9	3.37 (1H, dd, 10.6, 1.8)
25	73.1	
26	23.3	1.17 (3H, s)
27	26.6	1.22 (3H, s)
28	65.2	3.44 (1H, d, 11.9) 3.73 (1H, d, 11.9)
29	15.9	1.08 (3H, s)
30	19.4	0.92 (3H, s)

and two hydroxymethyls [δ_H 3.44 (d, J = 11.9 Hz, H-29a), δ_H 3.75 (d, J = 11.9 Hz, H-29b); δ_H 3.77 (dd, J = 11.2 and 3.3 Hz, H-21a), and δ_H 3.60 (dd, J = 11.2 and 4.9 Hz, H-21b). The ^{1}H and ^{13}C NMR spectra were typical of triterpenes of the cycloartane series. The high field pair of doublets at δ_H 0.80 and 0.59 ppm with a geminal coupling constant (J = 4.2 Hz) was characteristic of this class of triterpenes.[14] The typical 3-keto carbonyl was found in the ^{13}C NMR spectrum at δ 218.6 ppm. Thus, **4** had the same basic skeleton as a previously reported cycloartane derivative,[15] with C-3 carbonyl and C-28 hydroxymethyl groups, but with a structurally different side chain at position C-17. The side chain moiety consisted of an OH-substituted quaternary carbon at C-25 (δ 73.1) with two geminal methyl groups (C-26 and C-27, δ_H 1.15 and 1.20, δ_C 23.3 and 26.6), a hydroxymethyl (C-21), a substituent instead of a secondary methyl group, along with a hydroxymethine at C-24 (δ_H 3.35, dd, J = 8.4 and 1.6 Hz; δ_C 78.8); therefore, **4** was assigned the structure 21,24,25,28-tetrahydroxycycloarten-3-one.

The relative configuration of **4** was determined on the basis of NOESY correlations depicted in Fig. 4. NOESY correlations showed that the relative configuration of the basic skeleton of **4** was similar to that of the aforementioned compound isolated by Li *et al.*[15] Recently, the differentiation of 24*R*- and 24*S*-stereoisomers of cycloartane-type triterpenes using ^{13}C NMR techniques have been reported.[16] The chemical shift of C-24 of 24*R*-type compound was at δ_C 79.6 and that of the *S*-type compound was at δ_C 78.8 in $CDCl_3$. C-24 of **4** resonated at δ_C 78.8; thus, the configuration

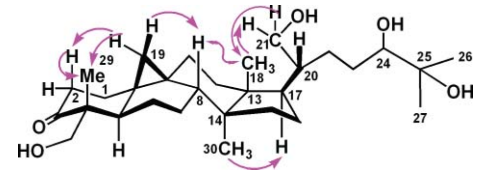

Fig. 4 Selected NOESY correlations of **4**.

of **4** was deduced as 24*S*, and determined as (24*S*)-21,24,25,28-tetrahydroxycycloartane-3-one.

Compounds **5–11** were isolated as known compounds, and their structures were determined by comparing the NMR data with those in the literature. Compounds **5–7** were determined as *ent*-13-*epi*-manool,[17] kaur-15-en-17-ol,[18] and *ent*-2β-hydroxymanool,[19] respectively. Compounds **8** and **9** were rocagloic acid derivatives and were determined as 1-*O*-formylrocagloic acid and 3′-hydroxyrocagloic acid, respectively, including absolute stereochemistry.[11] Compounds **10** and **11** were identified as dasyclamide[20] and 2β,15-dihydroxy-*ent*-labda-8(17),13*E*-diene,[21] respectively. Of the isolates, **8** and **9** were previously isolated from this plant, whereas others were isolated for the first time from this plant.

The isolated compounds (**1–11**) were evaluated for their activity in overcoming TRAIL resistance in AGS cells. As shown in Fig. 5A, treatment with 100 ng mL^{-1} TRAIL for 24 h resulted in only a slight decrease in cell viability (91 ± 4.5%). Luteolin,[5] used as a positive control, produced about 62% more inhibition along with TRAIL than the agent alone at 17.5 μM. Treating cells with 1.25 or 2.5 μM of **1** along with TRAIL (100 ng mL^{-1}) resulted in 45 and 57% more inhibition than the agent alone, showing its strong activity in overcoming TRAIL resistance. Treating cells with 100 ng mL^{-1} TRAIL and 1 or 2 nM of **8** reduced cell viability to 68 ± 5% and 36.5 ± 1.3% of control levels ($p < 0.01$), respectively,

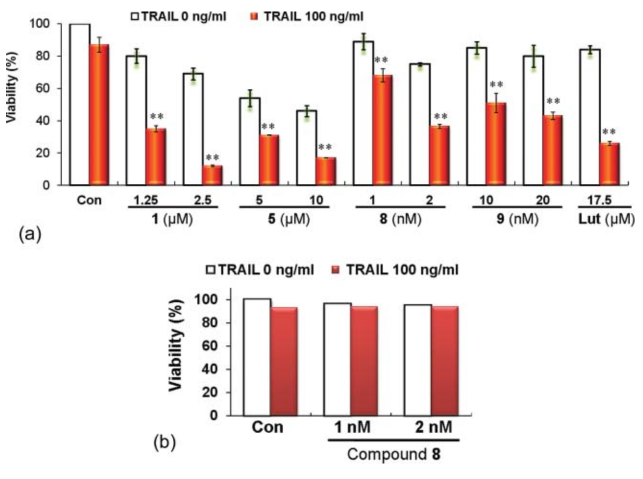

Fig. 5 (A) Effect of compounds **1**, **5**, **8**, **9**, and luteolin (positive control: Lut) and TRAIL treatment, alone and in combination, on the viability of AGS cells. (B) Effect of **8** and TRAIL treatment, alone and in combination, on cell growth of human renal epithelial (293T) cells. Cells were seeded in a 96-well culture plate (6 × 10^3 cells per well) for 24 h and then treated with indicated concentrations of the compounds and TRAIL (100 ng mL^{-1}) for 24 h. Cell viability was determined by Fluorometric Microculture Cytotoxicity Assay (FMCA). Bars represents the mean (n = 3 ± SD). Significance was determined by Student's t-test $p < 0.01$ (**) *vs.* control (Con).

which was 24 and 38% more than the agent alone, showing its strong activity in overcoming TRAIL resistance. Treating cells with 100 ng mL^{-1} TRAIL and 10 or 20 nM of **9** resulted in 33 and 37% more inhibition than the agent alone, indicating its strong activity. Combined treatment of TRAIL and **5** (5 or 10 μM) resulted in 23 and 29% more inhibition than the agent alone, indicated its moderate activity in overcoming TRAIL resistance. Compounds **2**, **3**, **4**, **6**, **7**, **10**, and **11** along with TRAIL did not produce any significant reduction in cell viability, suggesting their inactivity in overcoming TRAIL resistance. It was evident from the results that compound **8** showed the most potent activity in overcoming TRAIL resistance in AGS cell lines.

To find out whether it exerted any cytotoxicity on normal cells, we then examined the effect of combined treatment of TRAIL (100 ng mL^{-1}) and **8** (1 or 2 nM) on human renal epithelial cell lines (293T), which showed no effect (Fig. 5B); thus, it can be concluded that **8** decreased cell viability selectively in AGS cancer cells without affecting normal 293T cells.

To ascertain whether the decrease in cell viability produced by the combined treatment of TRAIL and **8** was caused by apoptotic cell death, we checked the treated cells displaying apoptotic morphology by Hoechst staining. After 24 h treatment with **8** and/or TRAIL, AGS cells were observed under a fluorescence microscope. We observed an increased number of cells with apoptotic nuclei in cells treated with **8** (1 and 2 nM) and TRAIL (100 ng mL^{-1}). The apoptotic nuclei contained fragmented chromatins stained more brightly in these cells than normal cells.[22] As shown in Fig. 6, no cells with apoptotic nuclei were found in control cells. These results indicated that the cell growth inhibition produced by the combined treatment of **8** and TRAIL was due to apoptosis.

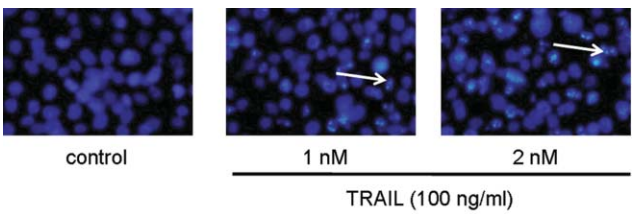

Fig. 6 Effect of combined treatment of **8** and TRAIL on apoptosis in AGS cells. AGS cells were grown on cell culture glass-bottom dishes and treated as described in the 'Experimental' and apoptosis was determined by Hoechst 33342 stain. Representative photomicrographs from each treatment group showing induction of apoptosis (bright fluorescence) marked by an arrow.

To determine whether the apoptosis enhanced by **8** was mediated *via* a caspase cascade, we first measured the activation of caspase-3 by a luminescent assay. Caspase-3/7 are known as effector caspases, and after being activated by initiator caspases (Caspase-8/9), they induced apoptosis. As shown in Fig. 7, combined treatment of **8** and TRAIL caused pronounced activation of caspase-3 in a dose-dependent manner. The results showed that combined treatment of **8** at 1 and 2 nM along with TRAIL (100 ng mL^{-1}) increased caspase-3/7 activity by 2.2- and 2.4-fold, respectively, of that of the control after 12 h. These results indicated that TRAIL-induced apoptosis enhanced by **8** involved the activation of caspase-3/7.

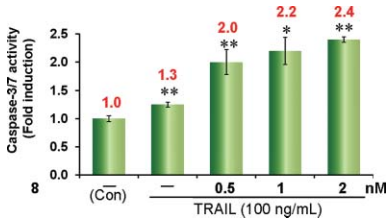

Fig. 7 Effect of **8** and TRAIL treatment on caspase 3/7 activity. AGS cells were treated with the indicated concentrations of **8** and TRAIL for 12 h. Activity was measured using the Caspase-Glo 3/7 assay kit. Values above columns are relative fold induction compared to the control ($n = 3$). Significance was determined with Student's *t*-test (**, $p < 0.01$; *, $p < 0.05$ *vs.* control).

To understand the molecular mechanism underlying the apoptosis produced by combined treatment of TRAIL and **8** in AGS cells, we next investigated changes in the expression of the death receptor pathway-related gene using real-time quantitative RTPCR analysis. The TRAIL-mediated apoptotic pathway begins with the binding of TRAIL to the death receptors DR4/DR5,[1] and we checked both DR4 and DR5 gene expression in AGS cells 3 and 6 h after treatment with compound **8**. As shown in Fig. 8, treatment of AGS cells to **8** upregulated the mRNA expression of both DR4 and DR5 after 3 and 6 h of treatment. **8** enhanced DR4 mRNA expression 1.68- and 1.64-fold compared to the control, after 3 h, at 1 and 2 nM, respectively. After 6 h, it caused 1.31-fold induction of DR4 mRNA expression at 2 nM (Fig. 8a). It also significantly enhanced gene expressions of DR5 by 1.42- and 1.32-fold, after 3 and 6 h, respectively, at 2 nM (Fig. 8b). The enhancement effect of **8** on DR4 and DR5 mRNA expression after 3 and 6 h of treatment correlated well with the caspase-3/7

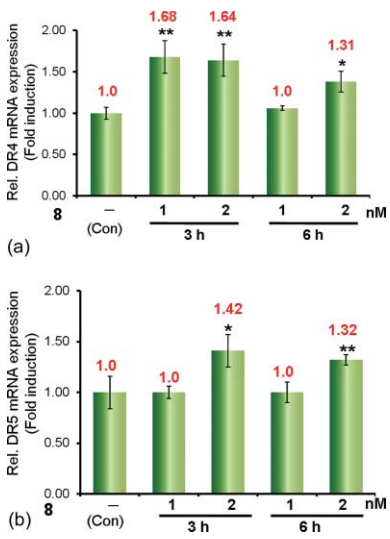

Fig. 8 Effect of **8** on DR4 (A) and DR5 (B) mRNA expression in AGS cells. AGS cells were treated with the indicated concentrations of **8**, and the expression was determined by real-time RT-PCR. The relative quantification of the target gene expression was normalized to the mRNA expression of an endogenous reference gene, GAPDH. Values above columns are the relative fold induction compared to the control ($n = 9$). The significance of differences was determined with Student's *t*-test (**, $p < 0.01$; *, $p < 0.05$ *vs.* control).

activity after 12 h and sensitization of cells to TRAIL-induced apoptosis after 24 h treatment.[23]

From the above results, it was evident that upregulation of DR4 and DR5 expression played a significant role in the apoptosis induced by combined treatment of **8** and TRAIL against TRAIL-resistant cells. Accordingly, to clarify the functional role of DR4 and/or DR5 upregulation, we investigated the effect of combined treatment of **8** and TRAIL on cell viability using recombinant human DR4/Fc and DR5/Fc chimera proteins, which have a dominant-negative effect by competing with endogenous DR5 and DR4, respectively.[6] As shown in Fig. 9, addition of 2.5 μg mL^{-1} DR4/Fc chimera blocked the cell death induced by combined treatment. Similarly, DR5/Fc chimera proteins also suppressed cell death with combined treatment of AGS cells with **8** and TRAIL. These results collectively indicated that upregulation of the death receptors is important for enhancement of TRAIL-induced apoptosis by **8**.

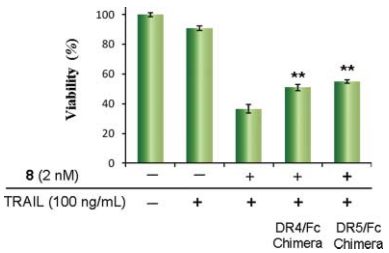

Fig. 9 TRAIL-induced cell death, enhanced by the combined treatment of **8** and TRAIL, was inhibited by DR4/Fc chimera and DR5/Fc chimera proteins. Significance was determined by Student's *t*-test (**, $p < 0.01$ *vs.* combined treatment of **8** and TRAIL) ($n = 3$).

Compound **8**, a rocagloic acid derivative containing a cyclopenta[b]benzofuran ring skeleton, was previously reported for its potent cytotoxic activity against a variety of tumor cells.[11] In addition, other rocagloic acid derivatives, as rocaglamide, silvestrol, *etc.*, were reported for their cytotoxic activity against several cancer cells.[24–27] Silvestrol, a potential anticancer rocaglate derivative from *Aglaia foveolata*, was reported to induce apoptosis in LNCaP cells through the mitochondrial/apoptosome pathway.[28] Here, we found for the first time its TRAIL resistance-overcoming activity in AGS cell lines with no effect on normal human (293T) cells; it sensitizes AGS cells to TRAIL by upregulating both DR4 and DR5 mRNA expression.

Experimental

General

UV spectra were obtained on a Shimadzu UV mini-1240 spectrometer. Optical rotations were measured with a JASCO P-1020 polarimeter. IR spectra were measured on ATR on a JASCO FT-IR 230 spectrophotometer. NMR spectra were recorded on JEOL A 500 and ECP 600 spectrometers with deuterated solvents, the chemical shift of which was used as an internal standard. FABMS was measured on a JEOL JMS-AX500 and HR-FABMS using a JEOL HX-110A spectrometer. HREIMS was measured on a JEOL JMS-GC Mate and HR-ESIMS using an Exactive spectrometer.

Plant material

The leaves of *A. cucullata* were collected from the Sundarbans Mangrove Forest, Bangladesh in November 2008, and were taxonomically identified by Prof. A. K. Fazlul Huq, Forestry and Wood Technology Discipline, Khulna University, Bangladesh. A voucher specimen was also deposited there for future reference (F018). Air-dried plants were ground before extraction.

Extraction and isolation

Dried, ground leaves of *A. cucullata* (280 g) were extracted with MeOH for 2 days at room temperature followed by homogenization and filtration, and then underwent evaporation and vacuum desiccation to obtain the crude extract (26 g). The extract was then chromatographed on Diaion HP-20 (4.5 × 35 cm; particle size 250–850 μm) to exclude the chlorophyll content. The chlorophyll-free fraction (19.3 g) was then suspended in 10% aq. MeOH (400 mL) and partitioned between hexane, EtOAc, and BuOH (350 mL × 4) to obtain the corresponding extracts. EtOAc extract (3.3 g) was subjected to silica gel PSQ100B column chromatography (2.5 × 54 cm) using the $CHCl_3$–MeOH solvent system with increasing polarity to afford fractions 2A–2G. Fraction 2B (17 mg) was subjected to preparative HPLC [Inertsil ODS·3, 1.0 × 25 cm; MeOH–H_2O (9 : 1); flow rate: 1.5 mL min^{-1}; RI and UV detection at 254 nm] to get compounds **2**, **3**, **5**, and **6** (t_R 30, 32, 40, and 45 min for compounds **2**, **3**, **5**, and **6**, respectively). Fraction 2D (319 mg) was chromatographed on silica gel 60 N (2.5 × 40 cm) using the hexane–acetone solvent system (13 : 1 → 0 : 1) to afford fractions 3A–3E. Fraction 3B was determined as compound **7** (4.1 mg). Fraction 3D (89.4 mg) was subjected to silica gel 60 N column chromatography (2.5 × 40 cm) using the hexane–acetone solvent system (7 : 1 → 0 : 1) to afford fractions 4A–4D. From 4C (13.6 mg), compound **8** (3.5 mg) was obtained after Sephadex LH20 column chromatography using MeOH as the eluent. Fraction 2F (193 mg) was subjected to silica gel 60 N column chromatography (2.5 × 40 cm) using the $CHCl_3$–MeOH solvent system with increasing polarity to afford fractions 5A–5E. From 5B (14 mg), compounds **1** (1.5 mg) and **4** (2.4 mg) were obtained after ODS flash column chromatography using 75% MeOH. Fraction 5D (54 mg) was subjected to silica gel 60 N column chromatography (1.5 × 40 cm) using the hexane–acetone–MeOH solvent system with increasing polarity (5 : 1 : 0 → 0 : 1 : 1) to afford fractions 6A–6E. From 6C (3.0 mg) and 6D (2.2 mg), compounds **9** (1.0 mg) and **10** (0.8 mg), respectively, were obtained after Sephadex LH20 column chromatography using MeOH as the eluent. Hexane extract (920 mg) was chromatographed over silica gel PSQ100B (2.0 × 60 cm) using the hexane–acetone–MeOH solvent system with increasing polarity to afford fractions 7A–7E. Compound **11** (8.4 mg) was isolated from fraction 7C (53 mg) after ODS flash column chromatography using 75% MeOH as the eluent.

Compound 1. Colorless solid; $[\alpha]_D^{17}$ −63.1 (*c* 0.1, $CHCl_3$); UV (MeOH) λ_{max} 253 nm (log ε 3.6); CD (MeOH) λ_{ext} nm (Δε) 253 (−9.1), 280 (+3.8); IR (ATR) ν_{max} 3362 (br), 2931, 1684, 1618, 1515, 1101, and 753 cm^{-1}; For ^{1}H and ^{13}C NMR data, see Table 1; HRESIMS *m/z* 667.2601 [M + Na]$^+$ (calcd for $C_{36}H_{40}N_2O_9Na$, 667.2626).

Compound 2. Colorless solid; $[\alpha]_D^{24}$ −58.1 (*c* 0.27, $CHCl_3$); UV (EtOH) λ_{max} 208 nm (log ε 3.7); IR (ATR) ν_{max} 3363 (br), 2937, 1715, 1643, 1458, and 1031 cm^{-1}; For ^1H and ^{13}C NMR data, see Table 2; HREIMS *m/z* 288.2468 M^+ (calcd for $C_{20}H_{32}O$, 288.2453).

Compound 3. Colorless solid; $[\alpha]_D^{24}$ −70.5 (*c* 0.13, $CHCl_3$); UV (EtOH) λ_{max} 208 nm (log ε 4.0); IR (ATR) ν_{max} 3411 (br), 2935, 1709, 1641, 1032, 889, 754 cm^{-1}; For ^1H and ^{13}C NMR data, see Table 2; HREIMS *m/z* 288.2445 M^+ (calcd for $C_{20}H_{32}O$, 288.2453)

Compound 4. Colorless solid; $[\alpha]_D^{21}$ +25.8 (*c* 0.2, $CHCl_3$); UV (EtOH) λ_{max} 204 nm (log ε 3.8); CD(MeOH) λ_{ext} nm (Δε) 204 (–0.3) and 207 (–0.6); IR (ATR) ν_{max} 3411 (br), 2935, 1709, 1641, 1032, and 754 cm^{-1}; For ^1H and ^{13}C NMR data, see Table 3; HRESIMS *m/z* 513.3546 $[M+Na]^+$ (calcd for $C_{30}H_{50}O_5Na$, 513.3550).

Cell cultures

AGS cells were derived from Institute of Development, Aging and Cancer, Tohoku University; cells were cultured in RPMI-1640 medium (Wako) with 10% FBS. Cultures were maintained in a humidified incubator at 37 °C with 5% CO_2.

TRAIL resistance-overcoming activity

TRAIL resistance-overcoming activity of the isolated compounds was assessed by comparing cell growth inhibitory activity in the presence and absence of TRAIL against TRAIL-resistant human gastric adenocarcinoma (AGS) cell lines.[29,30] AGS cells were seeded in a 96-well culture plate (6×10^3 cells per well) in 200 μL RPMI medium containing 10% FBS. Cells were incubated at 37 °C in a 5% CO_2 incubator for 24 h. Test samples with or without TRAIL (100 ng mL^{-1}) at different doses were then added to each well. After 24 h incubation, the cells were washed with PBS, and 200 μL PBS containing fluorescein diacetate (10 μg mL^{-1}) was added to each well. The plates were then incubated at 37 °C for 1 h, and fluorescence was measured in a 96-well scanning spectrofluorometer at 538 nm, following excitation at 485 nm.

Hoechst staining

Apoptosis was detected by staining the treated cells with Hoechst 33342 reagent (Wako Pure Chemical Industries Ltd., Japan) as described previously.[22,23] Briefly, AGS cells (2.5×10^5 cells), suspended in 2 mL RPMI 1640 medium, were seeded on a 3.5 cm glass-bottomed cell culture dish. After 24 h incubation, the cells were treated with 1 and 2 nM of compound **8** and TRAIL (100 ng mL^{-1}), respectively, for 24 h. Hoechst 33342 reagent was then added to each dish (20 μL), incubated at 37 °C, and observed under a fluorescence microscope (OLYMPUS DP72, Japan). Photographs of the stained cells were scanned by Flex Scan S1721.

Caspase-3/7 activity

Caspase-3/7 activity was measured using the Caspase-Glo 3/7 Assay kit (Promega) according to the manufacturer's instructions, as described previously.[6] Briefly, the cells were treated with 0.5, 1.0, and 2.0 nM of compound **8** and TRAIL (100 ng mL^{-1}) for 12 h, collected, and lysed. Cell lysates were incubated with a luminogenic substrate, z-DEVD-amino-luciferin at room temperature for 1 h and luminescence was monitored using a luminometer (Luminoskan Ascent, Thermo Electron Corporation, Japan).

Real-time RT-PCR analysis

Total RNA was extracted from AGS cells (2.5×10^5 cells) using TRIZOL reagent (Invitrogen), according to the manufacturer's instructions.[31,32] cDNAs were synthesized from 1 μg total RNA using the SuperScript III Platinum SYBR Green Two-Step qRT-PCR Kit (Invitrogen), as recommended by the supplier. Template cDNA thus obtained was incubated with 200 nM gene-specific primers (Fasmac) and with a SuperScript III Platinum Two-Step qRT-PCR kit with SYBR Green (Invitrogen) in a Mx3000 QPCR System (Stratagene). The thermal cycling program had initial incubation (50 °C for 2 min) and initial denaturation (95 °C for 2 min) and then 40 cycles of denaturation (95 °C for 15 s), annealing and extension (60 °C for 30 s). The primer sets used were as follows: glyceraldehydes-3-phosphate dehydrogenase (GAPDH), 5′-ATGGGGAAGGTGAAGGTCG-3′ and 5′-TAAAAGCAGCCCTGGTGACC-3′; DR5, 5′-GAGCTAAGTCCCTGCACCAC-3′ and 5′-AATCACCGACC-TTGACCATC-3′; DR4, 5′-GGAACTTTCCGGAATGACAA-3′ and 5′-GTCACTCCAGGGCGTACAAT-3′. The fluorescence signal was collected at the end of each cycle. After the reactions were terminated, the signal at each temperature from 60 °C to 95 °C was also collected for dissociation curve analysis. All reactions were performed in triplicate to confirm reproducibility, and the amount of target mRNA in each sample was normalized with that of mean GAPDH, an endogenous control.[6]

Acknowledgements

This work was partly supported by a Grant-in-Aid for Scientific Research from the Japan Society for the Promotion of Science (JSPS).

References

1 M. Ishibashi and T. Ohtsuki, *Med. Res. Rev.*, 2008, **28**, 688–714.
2 L. Zhang and B. Fang, *Cancer Gene Ther.*, 2005, **12**, 228–237.
3 D. R. Camidge, *Clin. Lung Cancer*, 2007, **8**, 413–419.
4 S. Baritaki, S. Huerta-Yepez, T. Sakai, D. A. Spandidos and B. Bonavida, *Mol. Cancer Ther.*, 2007, **6**, 1387–1399.
5 M. Horinaka, T. Yoshida, T. Shiraishi, S. Nakata, M. Wakada, R. Nakanishi, H. Nishino, H. Matsui and T. Sakai, *Oncogene*, 2005, **24**, 7180–7189.
6 T. Ohtsuki, H. Kikuchi, T. Koyano, T. Kowithayakorn, T. Sakai and M. Ishibashi, *Bioorg. Med. Chem.*, 2009, **17**, 6748–6754.
7 A. K. Das, I. Z. Shahid, M. S. K. Choudhuri, J. A. Shilpi and F. Ahmed, *Orient. Pharm. Exp. Med.*, 2005, **5**, 37–42.
8 K. R. Kirtikar and B. D. Basu, *Indian Medicinal Plants*, International Book Distributors, India, 1999, pp 553–554.
9 A. K. Das, I. Z. Shahid, F. Ahmed, M. Moniruzzaman and M. M. Masud, *Dhaka Univ. J. Pharm. Sci.*, 2005, **4**, 83–85.
10 U. C. Basak, A. B. Das and P. Das, *Bull. Mar. Sci.*, 1996, **58**, 654–659.
11 P. Chumkaew, S. Kato and K. Chantrapromma, *Chem. Pharm. Bull.*, 2006, **54**, 1344–1346.
12 A. A. Salim, H. B. Chai, I. Rachman, S. Riswan, L. B. Kardono, N. R. Farnsworth, E. J. Carcache-Blanco and A. D. Kinghorn, *Tetrahedron*, 2007, **63**, 7926–7934.
13 J. A. Garbarino, M. C. Chamy, M. Piovano, L. Espinoza and E. Belmonte, *Phytochemistry*, 2004, **65**, 903–908.
14 S. Weber, J. Puripattanavong, V. Brecht and A. W. Frahm, *J. Nat. Prod.*, 2000, **63**, 636–642.

15 F. Li, S. Awale, H. Zhang, Y. Tezuka, H. Esumi and S. Kadota, *J. Nat. Prod.*, 2009, **72**, 1283–1287.
16 M. D. Greca, A. Florentino, P. Monaco and L. Previtera, *Phytochemistry*, 1994, **35**, 1017–1022.
17 F. Nagashima, H. Tanaka and Y. Asakawa, *Phytochemistry*, 1996, **42**, 93–96.
18 G. Zhang, S. Shimokawa, M. Mochizuki, T. Kumamoto, W. Nakanishi, T. Watanabe, T. Ishikawa, K. Matsumoto, K. Tashima, S. Horie, Y. Higuchi and O. P. Dominguez, *J. Nat. Prod.*, 2008, **71**, 1167–1172.
19 F. Bohlmann, W. Kramp, M. Grenz, H. Robinson and R. M. King, *Phytochemistry*, 1981, **20**, 1907–1913.
20 Chaidir, W. H. Lin, R. Ebel, R. Edrada, V. Wray, M. Nimtz, W. Sumaryono and P. Proksch, *J. Nat. Prod.*, 2001, **64**, 1216–1220.
21 C. Zdero, F. Bohlmann and H. M. Niemeyer, *Phytochemistry*, 1990, **29**, 3247–3253.
22 V. M. Adhami, A. Malik, N. Zaman, S. Sarfaraz, I. A. Siddiqui, D. N. Syed, F. Afaq, F. S. Pasha, M. Saleem and H. Mukhtar, *Clin. Cancer Res.*, 2007, **13**, 1611–1619.
23 D. Llobet, N. Eritja, M. Encinas, N. Llecha, A. Yeramian, J. Pallares, A. Sorolla, F. J. Gonzalez-Tallada, X. Matias-Guiu and X. Dolcet, *Oncogene*, 2008, **27**, 2513–2524.
24 M. L. King, C.-C. Chiang, H.-C. Ling, E. Fugita, M. Ochiai and A. T. McPhail, *J. Chem. Soc., Chem. Commun.*, 1982, 1150–1151.
25 B. Cui, H. Chai, T. Santisuk, V. Reutrakul, N. R. Farnsworth, G. A. Cordell, J. M. Pezzuto and A. D. Kinghorn, *Tetrahedron*, 1997, **53**, 17625–17632.
26 T.-S. Wu, M.-J. Liou, C.-S. Kuoh, C.-M. Teng, T. Nagao and K.-H. Lee, *J. Nat. Prod.*, 1997, **60**, 606–608.
27 S.-K. Wang, Y.-J. Cheng and C.-Y. Duh, *J. Nat. Prod.*, 2001, **64**, 92–94.
28 S. Kim, B. Y. Hwang, B. N. Su, H. Chai, Q. Mi, A. D. Kinghorn, R. Wild and S. M. Swanson, *Anticancer Res.*, 2007, **27**, 2175–2183.
29 R. Larsson, J. Kristensen, C. Sandberg and P Nygren, *Int. J. Cancer*, 1992, **50**, 177–185.
30 F. Ahmed, T. Ohtsuki, W. Aida and M. Ishibashi, *J. Nat. Prod.*, 2008, **71**, 1963–1966.
31 P. Chomczynski and N. Sacchi, *Anal. Biochem.*, 1987, **162**, 156–159.
32 P. Chomczynski, *Biotechniques*, 1993, **15**, 532–537.